

# Analysis of impurities of Nd-Fe-B Magnet by nuclear method and recovery by precipitation chemical of Nd and Pr rare earths

K. Cheraitia<sup>a</sup>, A. Lounis<sup>a</sup> and M. Mehenni<sup>a</sup>

<sup>a</sup>Laboratory of Sciences and Material Engineering, University of Sciences and Technology, Houari Boumediene, BP32 El Alia, 16111 Algiers, Algeria.

Corresponding author: email: cheraitiak@yahoo.fr

Received date: January 08, 2017; revised date: April 10, 2017; accepted date: May 23, 2017

---

## Abstract

The products of the new information and communication technologies (NTIC), whose life often not exceed three years, became consumables to the computer image and other waste that contains neodymium and praseodymium (rare earths). In this field of analysis of impurities, treatment and recycling of waste, we propose the recovery of elements such as neodymium and praseodymium, from the super-magnet Nd-Fe-B. Our study provides a simple process and inexpensive. The implementation scheme of our project consists in a first step in developing a plan of experience that has been made specifically to perform the optimization of operating conditions of the precipitation process. This experimental design was inspired by a statistical technique advanced design of experiments known factorial design. The flow sheet processing of recovery begins by embrittlement in liquid nitrogen (-196°C) followed by dissolution in an acidic solution and precipitation of Nd as neodymium oxalate. For characterization we used the following techniques: The neutron radiography, the neutron activation analysis (NAA), the scanning electron microscope coupled with EDX and XRD. The counting of  $\gamma$  spectrum shows that the purity of the precipitate is higher than 99%. Then, the thermal decomposition transforms this powder to neodymium oxide. After the reduction we obtain pure neodymium

**Keywords:** Magnet analysis; rare earths; neutron activation analysis; neutron radiography; precipitation chemical; separation by solvent extraction;

---

## 1. Introduction

The development of the nuclear industry and the development of new separation techniques (ion exchange, solvent extraction) lanthanides compounds have become more common chemicals. The Lanthanides are considered important industrial materials by their specific characteristics. The specificity of rare earth is mainly due to the f electrons which gives them two essential properties: optical and magnetic. The rare earths are used to make magnetic alloys (neodymium-doped dysprosium) which play an important role in advanced technologies used in particular for wind turbines. Their magnetic properties, which depend on quantum characteristics, are exceptional: the f electrons are not involved in chemical bonds; they are free to participate in magnetism. The rare earth having these f electrons are difficult to separate because their numbers of electrons also affect their physical properties, which has an impact on their industrial interest [1, 2]. The rare earths have exceptional magnetic properties, their saturation magnetization is much higher than the iron one [3].

From raw material the composition is very complex. The steps that achieve different lanthanides as pure products are long, difficult and expensive [4-7]. The

dissolved lanthanides are separated from impurities by various reactions as the insolubility hydroxides, fluorides, oxalates, phosphates or alkali double sulfates [8-10]. In this context we would like to assess the degree of contamination of the magnet Nd-Fe-B, they have the highest magnetic field intensity. The demand for rare earth elements increases with 9-15% per year [11, 12]. The production of neodymium (Nd) has considerably increased since the development of neodymium-iron-boron (Nd-Fe-B) permanent magnet [13-14]. These magnets are found in almost all the NTIC products (New Technologies of Information and Communication). NTIC products whose life cycle does not usually exceed three years have become consumables. Just like the hard disks drive (HDD) in a personal computer, which contain neodymium and praseodymium [15]. The concept of sustainable development is invoked as a necessity for recycling materials. The waste from NTIC products has nevertheless a residual material value, compromised by the disassembly cost in the developed countries, but economic in developing or third world countries.

Our work has two stages. The first step is to determine the content of neodymium and the impurities of a magnet Nd-Fe-B. To do this we used the following techniques: The neutron radiography, the neutron activation analysis

(NAA) and the scanning electron microscope (SEM) coupled with EDX. Few studies mention the analysis of impurities in the magnets marketed. In a second step the powder (Nd-Fe-B magnet) is dissolved in hydrochloric acid solution. We add an oxalic acid solution to precipitate Nd as neodymium oxalate [4, 16]. The powder was analyzed by SEM/EDX and X-ray diffraction. The gamma ( $\gamma$ ) counting allows the determination of the content of neodymium, after oxalate precipitation and production of the Nd<sub>2</sub>O<sub>3</sub> powder [17].

## 2. Materials and methods

### 2.1. Neutron activation analysis

The neutron activation analysis is a method of making a sample radioactive by irradiation in a neutron field and thereafter one proceeds to identification via the energy emitted by the corresponding isotopes and their half life [18]. Samples of the Nd-Fe-B matrix and the standard were weighed, packaged, and irradiated simultaneously in the thermal reactor column under a neutron flux magnitude of  $5.4 \times 10^{12}$  n/cm<sup>2</sup>/s. The long irradiation was made in thermal column, with a magnitude of  $2.1 \times 10^{11}$  n/cm<sup>2</sup>/s for a time of 10 hours. At the end of the long irradiation, the samples were transferred directly to a shielded cell for 10 days decay time. The radioactivity of the samples was measured using a  $\gamma$  spectrometric chain which is composed of the following elements: germanium high purity detector (Hp/Ge) having a efficiency  $\epsilon = 1.2\%$ , and resolution of 1.80 keV. The ratio Pic/Compton is 40. These characteristics are measured for  $\gamma$  line at 1.33 MeV <sup>60</sup>Co. A preamplifier and an analyzer 8192 ORTEC channels incorporating an amplifier samples and standard were measured in the same counting geometries.

### 2.2. Neutron radiography

This technique is non-destructive analysis for the control and structural characterization of opaque or solid materials at the micrometer scale. In this work, we will apply the so-called transfer technique to obtain radiographs of super magnet, thereafter we will use digital processing techniques of the images obtained for qualitative operation to access information structures. In the transfer method only the converter is exposed to neutron beams and becomes radioactive. The intensity of the secondary radiation is proportional to the spatial neutron intensities. The converter is transferred after irradiation in the darkroom and placed in contact with a radiographic film. In this technique the gamma flux present in the beam does not interfere with the method.

### 2.3. Mass spectrometry

A small portion of the sample is transformed into ions. These ions are then subjected to electric and possibly

magnetic fields and their path will depend on the m/z ratio. After separation, the ions finish their path in a detector sensor. An analysis of the chemical composition of the samples was performed using a mass spectrometer SPECTRO MaxX.

### 2.4. Precipitation of neodymium

As extraction method we increased our choice of precipitation. We note in passing that the solubility of a metal (Neodymium), that is to say the neodymium concentration present in all its forms in the leaching solution, highly dependent on pH. Note also that the pH of maximum precipitation of metals does not coincide. It is therefore necessary to seek an optimum pH range to optimize removal of the desired metal. A wise choice provides a precipitate uncontaminated. Faced with changing regulations which requires severe concentration thresholds before discharge of the effluent, we must optimize returns from precipitation. The precipitation process is also influenced by other factors: choice of reagent, concentration of the precipitating agent, valence of the cation to eliminate proportion of cations, temperature, stirring speed. The optimum parameters are impossible to predict without resorting to preliminary tests. Subsequently mathematical modeling established between precipitation returns and levels of selected factor, the precipitation tests were performed according to a planning of experiments at three levels three ( $3^3$  or 27 experiments).

#### 2.4.1 Optimization of operating conditions

The goal is to have a minimum number of experiments to obtain the necessary information; this method reduces the confusion between the effects of different parameters. In addition, this method allows the simultaneous variation, systematic and effective in several settings at once. The aim of this experimental plan is to measure the causal relationships effect between the operating conditions and answers 'y' through the construction of an empirical model. This model can then be used to determine the minimum response "y" within the experimental range under observation, and the operating conditions to achieve it. After these experiments, it is possible to obtain a precipitation pattern of response to be optimized. This linear model has three settings and three variables each ( $3^3$ ): the influence of the three unit parameters, the three interactions of three factors lead to a total of 27 experiments. The three variables are: the concentration of Nd (0.001M, 0.003M, and 0.009M), the oxalic acid concentration of 0.5M, 1M and 0.75M and the pH of the solution 2.5, 3 and 3.5. Each parameter has three levels. Every time, it will be necessary, we adjust the pH with a sodium hydroxide solution. Depending on the experimental design, the mass balance of Nd -Fe-B powders 27 manipulation is performed. For this step we have plate and agitation motors, three Erlenmeyer flasks,

three beakers and three funnels and filter paper to perform the filtration.

An oven for drying and analytical balance for weighing the precipitate and calculate the returns of each precipitation assay. The addition of oxalic acid is carried out under stirring. Precise amounts of reagents are based on theoretical calculations in line with the following reaction:



To ensure the total recovery of Nd, is added drip to slightly exceed the theoretical amount calculated, After filtering the solution a drying to 70°C. This is done for 24 hours. The precipitate is weighed and stored.

### 2.5. Characterization

The resultant powder was characterized by using X-ray diffractometer carried out with X'Pert Pro MPD under Cu-K $\alpha$  radiation ( $\lambda=0.154$  nm). Microstructure and chemical composition of the samples were investigated by JSM-6360, JEOL scanning electron microscope (SEM) equipped with an energy dispersive X-ray (EDX) analyser at an accelerating voltage of 10-20 kV.

## 3. Results and discussion

The results of neutron activation are presented as intensity spectra of  $\gamma$  radiation as a function of energy. The methodology adopted in this work is to identify all the elements present in the sample. This step is very important because it allows us to identify short period elements. These elements become saturated quickly and therefore they require very short irradiation time. The long-period elements slowly reach saturation, they require higher fluence neutron irradiation. The qualitative analysis of elements is performed by short periods  $\gamma$  spectrometry. Induced activity in the sample is due to radioisotope production. When  $N_i$  stable atoms of a material are irradiated by a neutron flux  $\varphi$  (n/cm<sup>2</sup>/s) for a time  $dt$ , the number of radioactive atoms  $N_i$  formed is given by the equation (1). At the same time begin the disappearance decay of radioisotopes formed. The system of evolution equations is obtained by producing the balance production - disappearance in equation (2).

$$dN_i/dt = \sigma_i \cdot \varphi \cdot N_i \quad (1)$$

$$dN_i/dt = \sigma_i \cdot \varphi \cdot N_i - \sigma_d \cdot \varphi \cdot N_i - \lambda_i N_i \quad (2)$$

Where:

- $\sigma_i$  (cm<sup>2</sup>) the capture cross section of the radioisotope  $i$
- $N_i$  et  $N_d$  (at/cm<sup>3</sup>): density numbers respectively of the isotopes  $X_i$  and  $X_d$
- $\lambda_i$  (s<sup>-1</sup>): constant of radioactive decay of the radioisotope  $i$
- $\varphi$  (n/cm<sup>2</sup>/s): neutron flux

- $t$  (s): neutron irradiation time

With the following conditions at  $t=0$ ,  $N_i(0)=N_i^0$  and  $N_d(0)=0$ , the solution of the system of equations (1) and (2) is written:

$$N_1(t) = N_1^0 e^{-\sigma_1 \varphi t} \quad (3)$$

$$N_2(t) = \frac{m \cdot \xi \cdot N}{M_A} \quad (4)$$

Where:

- $m$ : mass of the sample
- $N$ : Avogadro's number
- $M$ : atomic mass,
- $\xi$ : isotopic enrichment

$$N_2(t) = \frac{\sigma_1 \cdot \varphi \cdot N_1^0}{\lambda_2 + (\sigma_1 - \sigma_2) \varphi} (e^{-\sigma_1 \cdot \varphi \cdot t} - e^{-(\lambda_2 + \sigma_2 \cdot \varphi) t}) \quad (5)$$

The activity  $A_2(t)$  is written:

$$A_2(t) = \lambda_2 \cdot N_2(t) \quad (6)$$

Asking  $\lambda_2 = \lambda_2 \cdot N_2 \cdot \sigma_2 \cdot \varphi$  equation (6) is written:

$$A_2(t_i) = \frac{\lambda_2 \sigma_1 \cdot \varphi \cdot N_1^0}{\lambda_2 - \sigma_1 \cdot \varphi} (e^{-\sigma_1 \cdot \varphi \cdot t_i} - e^{-\lambda_2 t_i}) \quad (7)$$

This relation is valid in most cases. However when it comes to a long irradiation for the elements with a large cross sections of absorption (high neutron flux), then take into account the consumption of target (burn-up).

For items with a large full resonance, consideration should account the fraction of the neutron spectrum located beyond the thermal field. The term  $\sigma \varphi$  will be replaced by  $(\sigma \varphi + I_0 \cdot \varphi_{epi})$

Where:

- $\varphi_{epi}$  is the epi-thermal neutron flux and  $I_0$ , the resonance integral (in barns).

The sample activity at the end of irradiation (at time  $t = t_i$ ) and after a time decrease  $t_d$  is given by equation (8).

$$A_2(t_i, t_d) = A_2(t_i) e^{-\lambda_2 t_d} \quad (8)$$

The cumulative activity of the sample after a time  $t_c$  count is:

$$A_2(t_i, t_d, t_c) = \int_0^{t_c} A_2(t_i, t_d) e^{-\lambda_2 t} dt \quad (9)$$

$$A_2(t_i, t_d, t_c) = \frac{\sigma_1 \cdot \varphi \cdot N_1^0}{\lambda_2} (1 - e^{-\lambda_2 t_i}) (1 - e^{-\lambda_2 t_c}) e^{-\lambda_2 t_d} \quad (10)$$

Determining the individual half-life of each radioelement is made by following the decrease of this one at constant time intervals. Table 1 provides the nuclear reactions used for sample analysis. The presence of specific radioisotopes is demonstrated in the  $\gamma$  spectra in Figure 2-5.

**Table1.** Nuclear reactions for sample analysis

Element	Target isotopes	Nuclear reactions	product	$\epsilon$ (%)	$\lambda$ (s <sup>-1</sup> )	$\gamma$ peak (KeV)
Nd	<sup>146</sup> Nd	<sup>146</sup> Nd (n, $\gamma$ ) <sup>147</sup> Nd	<sup>147</sup> Nd	17.2	7.30E-07	531
Fe	<sup>58</sup> Fe	<sup>58</sup> Fe (n, $\gamma$ ) <sup>59</sup> Fe	<sup>59</sup> Fe	0.28	1.68E-07	1099
Co	<sup>59</sup> Co	<sup>59</sup> Co (n, $\gamma$ ) <sup>60</sup> Co	<sup>60</sup> Co	100	3.79E-09	1173
		<sup>61</sup> Ni (n, p) <sup>60</sup> Co				
Al	<sup>28</sup> Al	<sup>28</sup> Al (n, $\gamma$ ) <sup>29</sup> Al	<sup>29</sup> Al	100	4.68E-03	1780
V	<sup>51</sup> V	<sup>51</sup> V (n, $\gamma$ ) <sup>52</sup> V	<sup>52</sup> V	99.75	2.8E-03	1435
Cu	<sup>63</sup> Cu	<sup>63</sup> Cu (n, $\gamma$ ) <sup>64</sup> Cu	<sup>64</sup> Cu	69.15	1.36E-05	511

For the three energy intervals, Figure 2 we can clearly infer the existence of elements that accompany Fe and Nd, these are: Al28, V52, Mn56, Cu66, Ge66, Ag108, Cs 136, Lu177m, Tb160, Re224, Bk246. Note also the presence of rare earth elements such as Dy160 and its isotope Dy165.

The elements of long period require very large irradiation time and do not appear on these spectra. The time counting of the vanadium element is taken as the reference time. The time decay of the respective elements will be determined from time decay vanadium which is given in table 2.

The energy measured by the neutron activation technique is confirmed by tables and energy isotopes. Tables 3 and 4 show the ratios of the matrix Nd-Fe-B obtained by neutron activation analysis, where all the elements short and long periods present appeared.

**Table2.** Reference time of the elements analyzed by NAA

Element	Decay time (s)
<b>Vanadium</b>	0
<b>Cooper/Manganese</b>	9035
<b>Neodymium</b>	18585
<b>Iron</b>	91534
<b>Nickel</b>	100219
<b>Nd-Fe-B Matrix</b>	169477
<b>Cobalt</b>	176891

**Table3.** Elements present in the Nd-Fe-B matrix after 2Min of a decay time

Probable radioisotope	Energy measured	Probable radioisotope	Energy measured
Ti-51	242	Lu-177m	54.07
Ni-65	55	Sm-153	69.67
Ni-65	181	J-131	80.18
In-116m	92	Eu-155	86.54
Ni-65	39	Cd-109	88.03
Cu-64	274	Nd-147	91.11
Ti-51	14	Np-239	99.55
Ni-65	24	Ta-182	100.11
In-116m	818.70	Sm-153	103.18
Mg-27	843.76	Gd-153	103.18
Mn-56	846.77	Np-239	103.76
Ni-65	852.70	Eu-155	105.31
Ti-51	928.63	Lu-177m	105.36
Ni-65	952.99	Np-239	106.12
In-116m	1096	Lu-177m	112.95
Cu-64	1346.55	Np-239	117
V-52	1434	Se-75	121.12
K-42	1523	Eu-152	121.78
Al-28	1778	Eu-154	123.07
Mn-56	1810.67	Ba-131	123.84

**Table4.** Elements present in the Nd-Fe-B matrix after 10 days of a decay time

Probable radioisotope	Energy measured	Probable radioisotope	Energy measured
Lu-177m	54.07	Ba-131	123.84
Sm-153	69.67	Yb-175	282.52
J-131	80.18	Pa-233	300.04
Eu-155	86.54	Se-75	303.92
Cd-109	88.03	Nd-147	319.41
Nd-147	91.11	La-140	432.49
Np-239	99.55	Nd-147	439.88
Ta-182	100.11	Hf-181	482.18
Sm-153	103.18	Ru-103	497.33
Gd-153	103.18	Cs-134	561.76
Np-239	103.76	Ga-72	600.95
Eu-155	105.31	Sc-46	889
Lu-177m	105.36	Tb-160	966.44
Np-239	106.12	Rb-86	1078
Yb-169	109.78	Ta-182	1121

The images obtained by neutron radiography are presented below in Figure1. The difference in contrast is due to the presence of the elements in the matrix Fe-Nd-B that does not absorb neutrons. We note that there are two colors, a dark which represents the clear film and the other representing the Fe-Nd-B matrix. The distribution of the components of the matrix is said to be homogeneous because the light portion of image shows that there is no chaotic distribution of these elements.

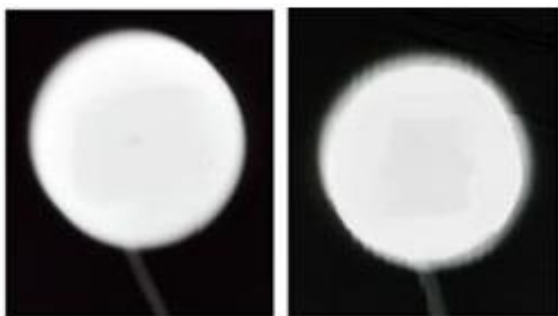


Figure1. Neutron radiography image of the Nd-Fe-B Matrix

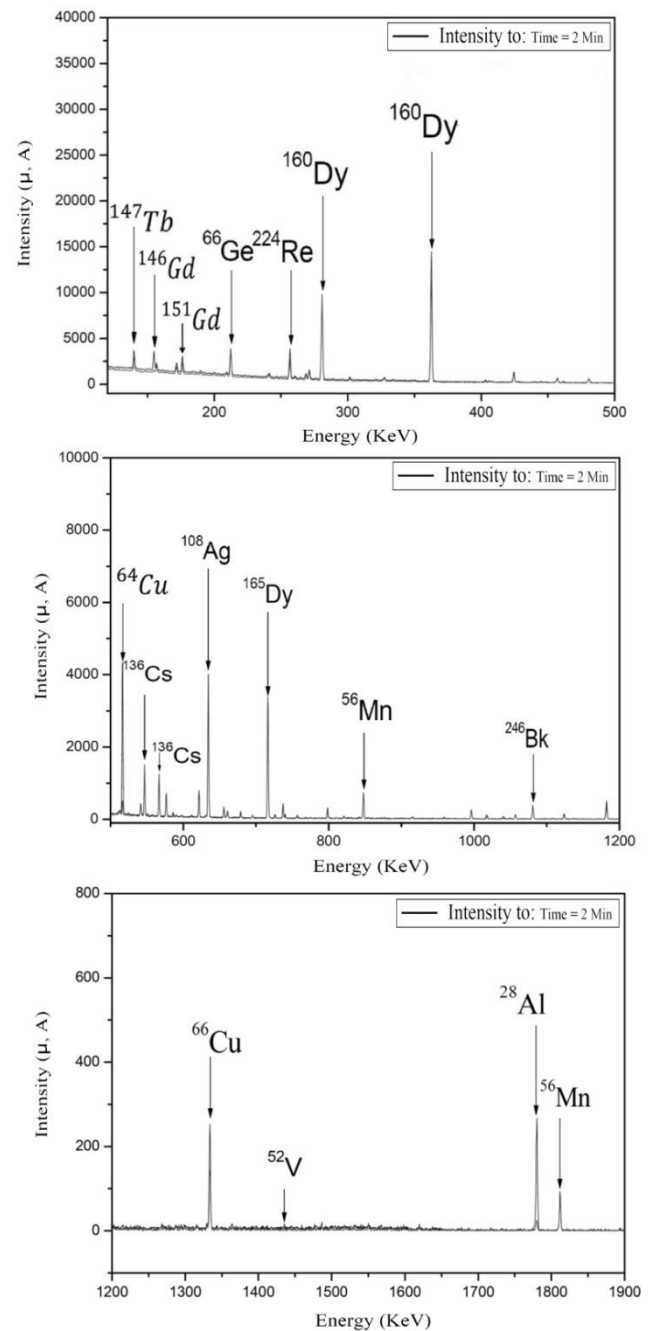


Figure2. Gamma spectra of the Nd-Fe-B Matrix: (a)100-500Kev.(b)500-1200Kev.(c)1200-1900Kev.

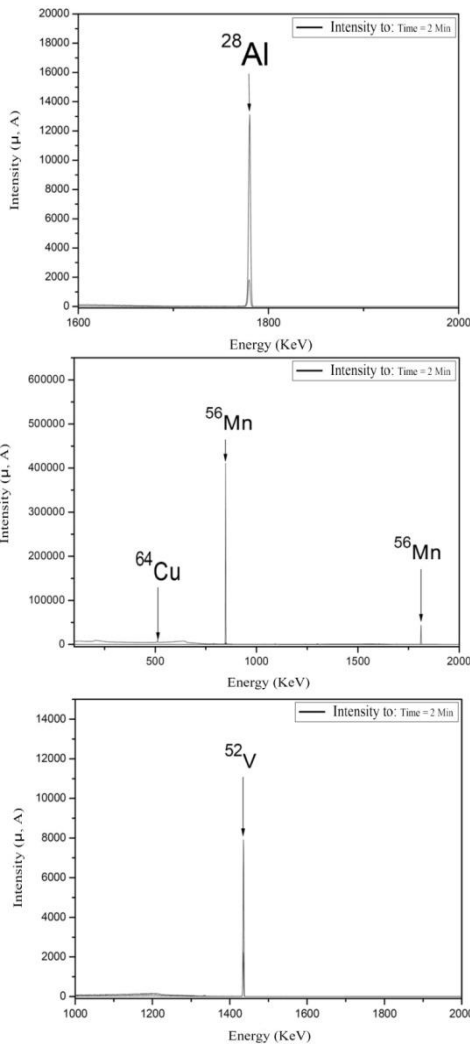


Figure3. Gamma spectra of the Standard sample:(a)1600-2000KeV. (b)120-2000KeV.(c)1000-2000KeV.

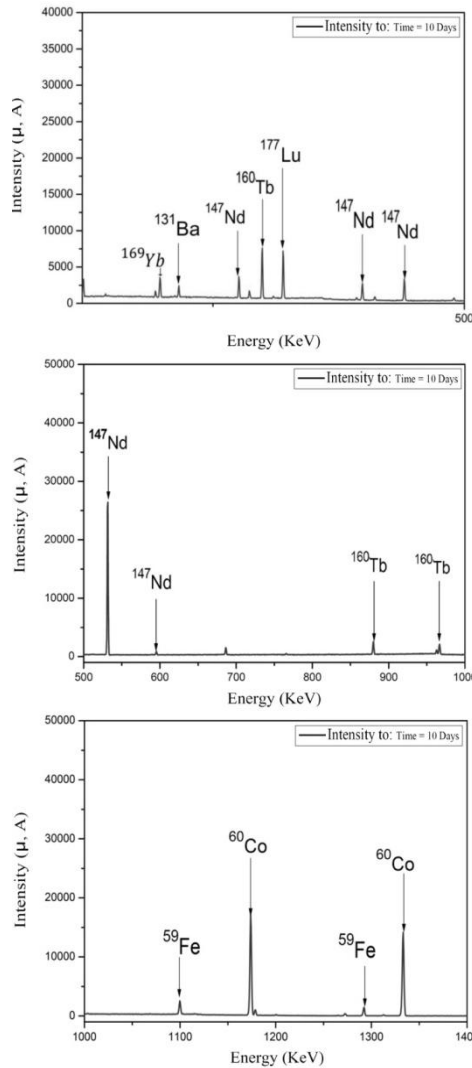


Figure4. Gamma spectra of the Nd-Fe-B Matrix: (a)100-500KeV. (b)500-1000KeV. (c)1000-1400KeV.

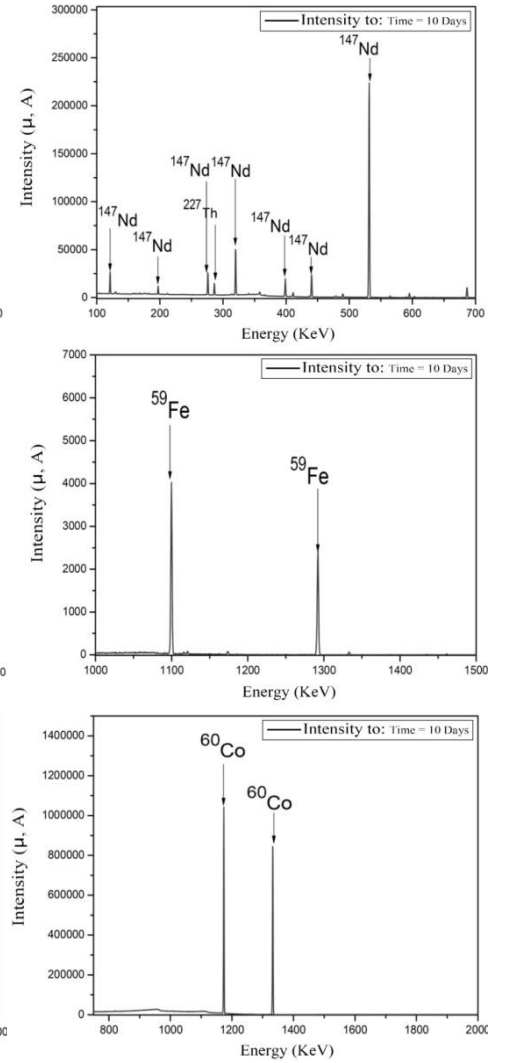


Figure5. Gamma spectra of the standard sample: (a)100-700KeV. (b)100-1500KeV. (c)750-2000KeV.

The micrographs (Fig. 6), shows the microstructure of Fe-Nd-B matrix, we can see the distribution of three different phases of contrast clear, gray, and black representing the iron, the neodymium and the boron. It is observed that the distribution of components is typical of a matrix of sintering materials. Neodymium grains are distributed between iron particle interstices. The particle distribution is uniform over the entire sample surface

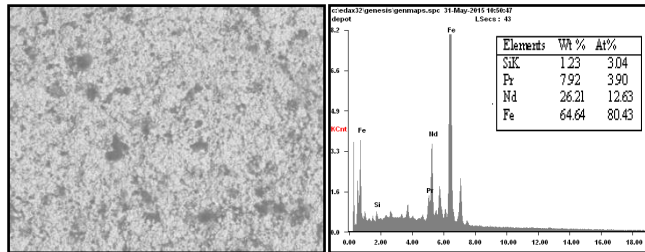


Figure6. Energy dispersive X-ray spectroscopy of the Nd-Fe-B Matrix

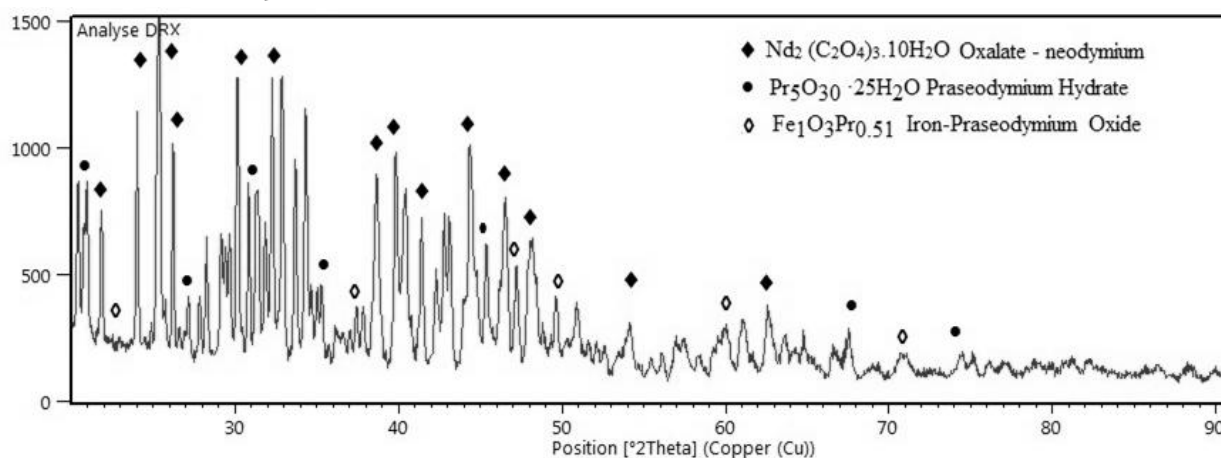


Figure7. XRD pattern for the neodymium oxalate

The result of chemical composition analysis for Nd<sub>2</sub>O<sub>3</sub> is in accord with XRD pattern (Fig.8) and micrographs SEM/EDX (Fig.9), in which the oxide of neodymium phase (hexagonal) is observed. The spectrum shows three intense peaks corresponding to the diffraction of the plans (110), (102) and (103). The presence of PrNdO<sub>4</sub> was also confirmed.

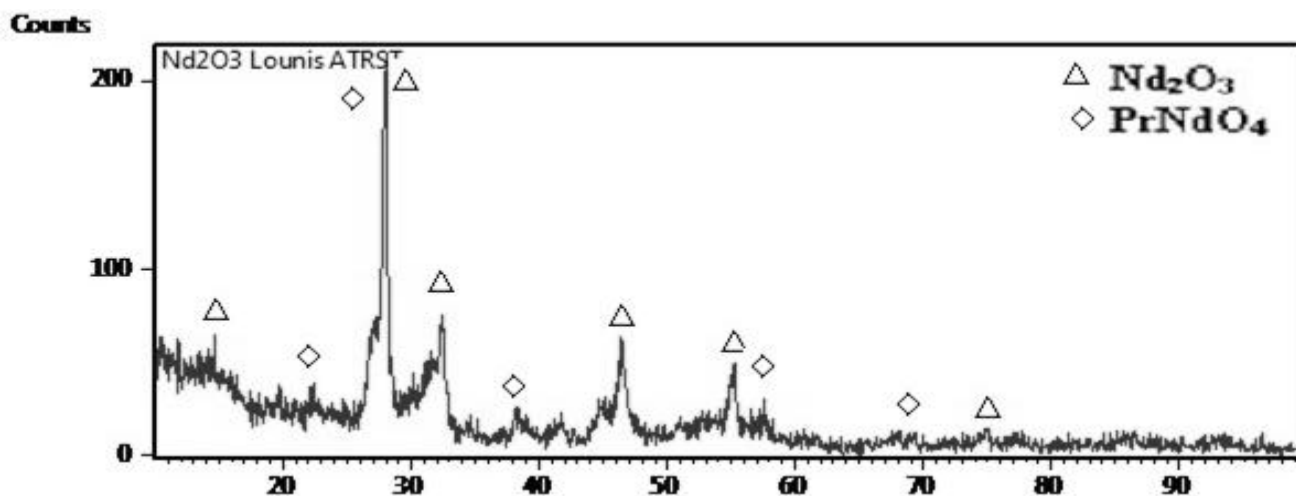
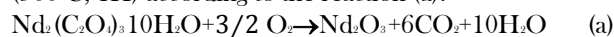


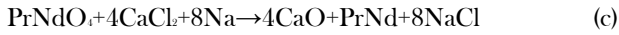
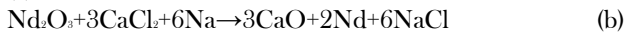
Figure 8. XRD pattern for the neodymium oxide

On the results of the precipitation tests: the best yield, 99% was obtained for [Nd]=0.003M, pH=3 and an oxalic acid concentration of 0.75M.

The obtained precipitate (neodymium oxalate) is analyzed: Identification of the three intense peaks of spectrum XRD (Fig.7) with cards ICDD, shows that three compounds are envisaged: the hydrated neodymium oxalate of Nd<sub>2</sub>C<sub>6</sub>H<sub>20</sub>O<sub>22</sub> chemical formula, praseodymium hydrate (FeO<sub>3</sub>Pr<sub>0.51</sub>), and iron-praseodymium oxide (Pr<sub>5</sub>O<sub>30</sub>.25H<sub>2</sub>O). The NAA shows that the precipitate contains 86.27% of neodymium and 13.72% of praseodymium and impurities. The thermal decomposition of this precipitate is carried out in a furnace (900°C, 1h) according to the reaction (a):



The last step is the reduction at 750°C of both oxides obtained previously. The choice of a reducer is conditioned initially by thermodynamic considerations resulting from the diagram of Ellingham, but also for kinetic and economic considerations. We chose CaCl<sub>2</sub> in the presence of sodium according to reaction (b) and (c):



The consideration of the diagrams of Ellingham is by the way when the difficulty of the reduction of oxides arises and in particular of metallic oxides in order to extract the elements. By taking into account the number of components, phases and equilibrium relations, the use of Gibbs phase rule gives a variance  $v = 1$ , therefore we have an invariant system. The control of the temperature is sufficient. After reduction the product obtained is analyzed by XRD. The results are given in Figure 10. The XRD spectrum of the obtained product shows the presence of CaO, Nd, NdPr and NaCl. Three intense peaks of neodymium, assigned to the diffraction of the planes (111), (200) and (220), corresponding to cubic structure and a lattice parameter of 0.48 nm.

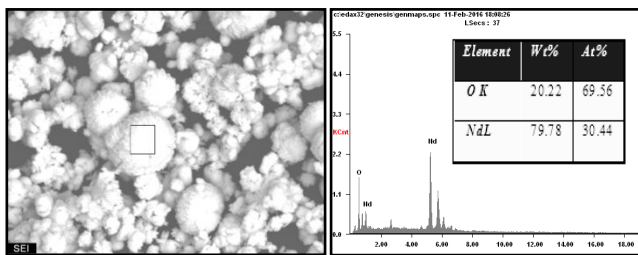


Figure9. Energy dispersive X-ray spectroscopy of the Nd<sub>2</sub>O<sub>3</sub>

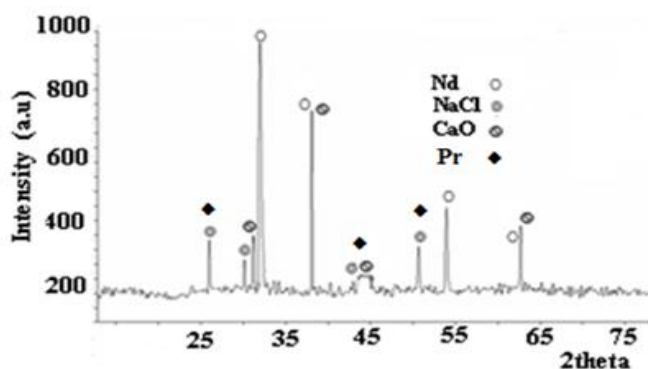


Figure10. XRD pattern reduction of neodymium oxide

#### 4. Conclusion

Our study concerns the recovery and analysis of rare earths from the electronic waste: this work has two stages. The implementation scheme of our project in particular has embrittlement in liquid nitrogen (-196°C), a dissolving in an acid and a recovery solution by unit operation of chemical engineering that will be followed by purification of neodymium and praseodymium. The first step is to determine the content of neodymium and the impurities of a magnet Nd-Fe-B. In a second step we add an oxalic acid to precipitate Nd as neodymium oxalate after dissolved the powder (Nd-Fe-B) in hydrochloric acid. For the determination of impurities in trace, neutron activation analysis is one of the few methods that achieves its theoretical limits of detection. His response times are dependent on the decay period of radioisotopes used and can reach several days. We have shown that this method can analyze trace and ultra-trace. From the same sample NAA gives us the ability to assay simultaneously a large number of elements present in the Nd-Fe-B alloy used as a super magnet. We can clearly infer the existence of elements that accompany Fe and Nd, these are: Al28, V52, Mn56, Cu66, Ge66, Ag108, Cs 136, Lu177m, Tb160, Re224, Bk246. On the results of the precipitation tests: the best yield, 99% was obtained for [Nd]=0.003M, pH=3 and an oxalic acid concentration of 0.75M. Another step of reduction at also been used with the Ellingham diagram, is to extractive metallurgy of reducing Nd<sub>2</sub>O<sub>3</sub> and PrNdO<sub>4</sub> so as to recover the metals namely Nd and Pr. The identification of the most intense peaks in the XRD spectrum shows the presence of a single compound which hydrated neodymium oxalate chemical formula Nd<sub>2</sub>(C<sub>2</sub>O<sub>4</sub>)<sub>3</sub>·10H<sub>2</sub>O. Its purity is measured by neutron activation analysis. The presence of PrNdO<sub>4</sub> was also confirmed. The result of chemical composition analysis for Nd<sub>2</sub>O<sub>3</sub> is in accord with XRD pattern and MEB/EDS in which the oxide of neodymium phase (hexagonal) is observed.

The processes of chemical precipitation, so the results that we found provide of real prospects for the recovery of rare earths from electronic waste

#### Acknowledgment

We acknowledge financial support from the Research Thematic Agency in Science and Technology. The authors are grateful for ATRST Algiers, Algeria.



**References**

- [1] M. Zakotnik, I.R. Harris, A.J. Williams. Multiple recycling of NdFeB-type sintered magnets, *Journal of Alloys and Compounds* 469 (2008) 314-321
- [2] C.Milmo. Concern as China clamps down on rare earth exports, 318, China 2010.
- [3] S. Ruoho. Modeling Demagnetization of Sintered NdFeB Magnet Material in Time-Discretized Finite Element Analysis, Department of Electrical Engineering, New York, USA, 2011.
- [4] B. Mokili, C. Potrenaud. Modelling of the extraction of Nd and Pr nitrates from aqueous solutions containing a salting-out agent or nitric acid by tri-n-butyl phosphate, *Journal of Solvent Extraction and Ion Exchange*. 14(4) (1996) 617.
- [5] T. Saito, H. Sato, T. Motegi. Recovery of rare earths from sludges containing rare-earth elements, *Journal of Alloys and Compounds*, 425 (2006) 145-147.
- [6] Y. Kanazawa, M. Kamitani. Rare earth minerals and resources in the world, *Journal of Alloys and Compounds* 408-412 (2006) 1339-1343.
- [7] S. Lalleman, M. Bertrand, E. Plasari. Physical simulation of precipitation of radioactive element oxalates by using the harmless neodymium oxalate for studying the agglomeration phenomena, *Journal of Crystal Growth*. 342 (2011) 42-49.
- [8] W. Yantasee, G.E. Fryxell, R.S. Addleman, R.J. Wiacek, V. Koonsiripaiboon, K. Pattamakomsan, V. Sukwarotwat, J. Xu, K.N. Raymond. Selective removal of lanthanides from natural waters, acidic streams and dialysate. *Journal of Hazard Mater.* 168 (2009) 1233-1238.
- [9] W H. Duan, P J.Cao, Y J.Zhu. Extraction of rare earth elements from their oxides using organophosphorus reagent complexes with HNO<sub>3</sub> and H<sub>2</sub>O in supercritical CO<sub>2</sub>, *Journal of Rare Earths*. 28(2) (2010) 221.
- [10] G.A. Moldoveanu, V.G. Papangelakis. Recovery of rare earth elements adsorbed on clay minerals. I. Desorption mechanism, *Journal of Hydrometallurgy*. 117-118 (2012) 71-78.168.
- [11] M. Zakotnik, I.R. Harris, A.J. Williams. Possible methods of recycling NdFeB-type sintered magnets using the HD/degassing process, Department of Metallurgy and Materials, University of Birmingham 450 (2007) 525-53.
- [12] T.Itakura, R. Sasai, H. Itoh. Resource recovery from Nd-Fe-B sintered magnet by hydrothermal treatment, *Journal of Alloys and Compounds*, 408-412 (2005) 1382-1385.
- [13] X Y.Du, T E.Graedel. Global rare earth in-use stocks in NdFeB permanent magnets, *Journal of. Ind. Ecol.* 15 (2011) 836.
- [14] J.H. Rademaker, R. Kleijn, Y.X. Yang. Recycling as a strategy against rare earth element criticality: a systemic evaluation of the potential yield of NdFeB magnet recycling, *Journal of Environ. Sci. Technol.* 47 (2013) 10129-10136.
- [15] T.H. Okabe, O. Takeda, K. Fukuda, Y. Umetsu. Direct extraction and recovery of neodymium metal from magnet scrap, *Journal of Materials Transactions* 44(4) (2003) 798.
- [16] T. Kobayashi, Y. Morita, M. Kubota. Development of Partitioning Method:Method of Precipitation Transuranium Elements with Oxalic acid", *JAERI-M88* (1988) 026.
- [17] J.W. Lyman, G.R. Palmer. Recycling of rare earths and iron from NdFeB magnet scrap, *Journal of High Temperature Materials and Processes*. 11(1-4) (2011) 175.
- [18] C. DE Wispelaere, J. P. OP DE Beeck, J. Hoste. Non-destructive determination of trace impurities in iron by thermal neutron activation analysis with long-LIVED ISOTOPES, Institute of Nuclear Sciences, Ghent University, Ghent, *Journal of Analytica ChiricaActa*. 64 (1973) 321-332.